EUROPEAN JOURNAL OF CANCER 42 (2006) 342–350

available at www.sciencedirect.com

SCIENCE DIRECT®

journal homepage: www.ejconline.com

Prospective comparison of the impact on treatment decisions of whole-body magnetic resonance imaging and computed tomography in patients with metastatic malignant melanoma

Christian Müller-Horvat[a,,1], Peter Radny[b,*,1], Thomas K. Eigentler[c], Jürgen Schäfer[a], Christina Pfannenberg[a], Marius Horger[a], Sascha Khorchidi[a], Thomas Nägele[d], Claus Garbe[c], Claus D. Claussen[a], Heinz-Peter Schlemmer[a]*

[a]*Department of Diagnostic Radiology, Eberhard-Karls-University, Tübingen, Germany*
[b]*Department of Dermatology, Albert-Ludwigs-University, Freiburg, Germany*
[c]*Department of Dermatology, Eberhard-Karls-University, Tübingen, Germany*
[d]*Department of Neuroradiology, Eberhard-Karls-University, Tübingen, Germany*

ARTICLE INFO

Article history:
Received 12 April 2005
Received in revised form
17 August 2005
Accepted 17 October 2005
Available online 20 December 2005

Keywords:
Whole-body MRI
Whole-body CT
Malignant melanoma

ABSTRACT

Patient management and treatment strategies for metastatic melanoma depend largely on the stage of metastatic disease. The aim of this study was to compare contrast-enhanced whole-body magnetic resonance imaging (wbMRI) and whole-body computed tomography (wbCT) to detect distant metastases for staging. A total of 43 patients (41 with completed wbCT and wbMRI examination) with known American Joint Committee on Cancer (AJCC) stage III–IV malignant melanoma were examined and 775 metastases were identified by both methods. Whole-body CT was able to detect 522 metastases, whereas wbMRI found 730 metastases. Whole-body CT identified 188 pulmonary metastases, compared with 143 metastases detected by wbMRI. In kidneys, adrenal glands and lymph nodes, respectively, wbCT and wbMRI detected the same number of lesions. Whole-body MRI detected more metastases than wbCT in liver (detection rate 122/199), spleen (26/54), subcutaneous tissue (39/61), muscle (4/11), bone marrow (23/132) and brain (15/25). Therapy was modified as a consequence of wbMRI findings in 10/41 (24%) patients. In conclusion, wbMRI detected clearly more malignant melanoma metastases in most organ systems with the exception of lung metastases. More accurate and complete staging by wbMRI has an impact on treatment strategy in about one-quarter of the patients.

* *Corresponding authors*: Tel.: + 49 7071 2980498; fax: + 49 7071 295392 (C. Müller-Horvat), tel.: +49 761 270 6701; fax: + 49 761 270 6665 (P. Radny).
E-mail addresses: christian.mueller@med.uni-tuebingen.de (C. Müller-Horvat), calvin32@gmx.de (P. Radny).
[1] Corresponding authors contributed equally.

0959-8049/$ - see front matter
doi:10.1016/j.ejca.2005.10.008

1. Introduction

Malignant melanoma is responsible for the majority of deaths due to skin cancer. During the past decades, the incidence of cutaneous melanoma has been rising continuously in both sexes in nearly all developed countries. In 2004, 55,100 new cases were expected in the United States of America (USA) [1]. The prognosis of cutaneous malignant melanoma is strongly related to the stage of the disease. The prognosis of advanced melanoma with visceral metastases is poor, with a 5-year survival of 5–14% [1,2].

To date, no sufficient treatment has been established for advanced melanoma [3]. Treatment with the single agent dacarbazine is considered to be a reference treatment for advanced melanoma. Response rates to dacarbazine and other chemotherapeutic treatments are low and of short duration. Therefore, the option of surgical metastasectomy is examined regularly and this indication depends on the chance to completely resect all recognisable metastases [4]. Complete identification of all organ metastases is a precondition for this invasive treatment strategy.

In daily routine staging, a variety of imaging techniques, such as computed tomography (CT) scan, ultrasound, scintigraphy, positron emitting tomography (PET) or part-body magnetic resonance imaging (MRI) is used and the combination of CT and PET (PET-CT) has also been introduced for clinical use. Recently, high-resolution whole-body MRI (wbMRI) became practical in one single examination by a method applying multiple phased array coils (up to 72) and receiver channels (up to 32) and using parallel imaging technology. In a first feasibility study, wbMRI was found to show great potential for the rapid assessment of individual tumour spread and total tumour burden during initial and follow-up staging examinations [5]. Different methods implemented earlier used either a moving table platform in combination with the body-coil or a specially designed rolling table platform with one body phased-array coil [6–8]. However, field-of-view, spatial and/or contrast resolution were slightly restricted compared with separately performed conventional state-of-the-art MRI examinations.

Here, we present the results of a prospective study investigating the efficacy of examinations with wbMRI compared with standard imaging with conventional whole-body (wb) spiral CT in 43 patients suffering from advanced malignant melanoma. Both techniques in each patient were applied consecutively after obtaining informed consent.

2. Patients and methods

2.1. Patient selection

After excluding contraindications to MRI (cardiac pacemaker, metal devices in the body, allergy to contrast medium, restricted renal function, pregnancy, claustrophobia) and CT (pregnancy, allergy against contrast medium, hyperthyreosis, restricted renal function), contrast-enhanced wbMRI and CT examinations were performed in patients with advanced metastatic cutaneous melanoma American Joint Committee on Cancer (AJCC) stage III–IV, which had to be staged in routine follow-up. A total of 43 patients were included in the study, but two patients refused the MRI examination due to claustrophobia. The Local Ethical Committee of the Medical Faculty of the University of Tübingen approved the study and patients gave their written consent after having been informed about the trial in detail.

All patients had to complete both examinations within 14 d in order to avoid changes in number and size of metastases due to progression or regression of the tumour between both examinations.

2.2. CT examination

For contrast-enhanced CT examinations a conventional spiral CT (Volume Zoom (4 row scanner), Somatom Sensation 16 (16 row scanner); Siemens AG, Erlangen, Germany) was used. Whole-body CT was performed in two separate examinations, first CT of the head (contrast medium (CM)-enhanced base, 120 kV, slice thickness 3 mm, in plane resolution about 4 mm; CM-enhanced cerebrum, 120 kV, slice thickness/reconstruction interval 9 mm/3 mm, in-plane resolution about 4 mm) and then CT of the liver (native, 120 kV, 80 mA, slice thickness/reconstruction interval 5 mm/5 mm, 0.75 collimation, in-plane resolution about 7 mm), of the thorax (CM-enhanced, 120 kV, 120 mA, first thickness/reconstruction interval 5 mm/5 mm, second thickness/reconstruction interval 10 mm/5 mm MIP THIN 3D-Mode, 1.5 collimation, in-plane resolution about 7 mm), of abdomen/pelvis (CM-enhanced, 120 kV, 140 mA, first thickness/reconstruction interval 5 mm/5 mm, second thickness/reconstruction interval 3 mm/2.5 mm 3D-Mode, 0.75 collimation, in-plane resolution about 7 mm) and of the neck (CM-enhanced, 120 kV, 200 mA, first thickness/reconstruction interval 4 mm/4 mm, second thickness/reconstruction interval 3 mm/3 mm 3D-Mode, 0.75 collimation, in-plane resolution about 4 mm). The amount of contrast medium was 150 ml + 50 ml, delay 35 s for thorax, 60 s for abdomen/pelvis and 25 s for neck. Distal femur with knee and the lower leg were not examined. The total examination time for CT from neck-thorax-abdomen-pelvis and CT from head lasted about 10–15 min.

2.3. MRI examination

For wbMRI examinations a novel whole-body 1.5 T system was used (Avanto, Siemens AG, Erlangen, Germany). Without repositioning of the patient a state-of-the-art MR imaging from head to toe is feasible using high-performance gradients (maximum amplitude: 45 mT/m; minimum rise time 200 μs, maximum slew rate 200 T/m/s), integrated parallel acquisition technique (iPAT) in three spatial directions and a total scan range of 205 cm by combining the large field-of-view (500 mm) with automatic table move. Whole-body MRI was performed in five subsequent table positions in the coronal direction (head/thorax; thorax/abdomen; pelvis; upper leg; lower leg) and in the axial direction (head; thorax; abdomen; pelvis). Additional contrast-enhanced MRI after intravenous application of Gadolinium-diethyltriaminepentaacetic acid (Gd-DTPA) (Magnevist, Schering, Berlin, Germany) was performed in the axial direction of the head, the thorax, the abdomen and the pelvis. The total examination lasted about 1 h. The complete wbMRI sequence protocol is shown in Table 1 and an example of images is shown in Fig. 1.

Table 1 – Magnetic resonance imaging (MRI) sequence protocol

Site	Sequences	Imaging plane	Spatial resolution (mm^3)	TR (ms)	TE (ms)	TI (ms)	Acquisition time (s)
Whole body	T2w STIR-TSE	Coronal	$1.8 \times 1.3 \times 5.0$	8540	87	150	877
Brain	Flair	Axial	$1.2 \times 0.9 \times 4.0$	8800	108	2500	160
	T1w-SE	Axial	$0.9 \times 0.9 \times 4.0$	500	7.8	–	183
Neck	STIR	Axial	$1.2 \times 0.9 \times 5.0$	6180	59	150	137
Thorax	T2w STIR-TSE (multi breath-hold)	Axial	$1.8 \times 1.2 \times 6.0$	3800	100	150	46
	T1w-VIBE 3D (breath-hold)	Axial	$2.0 \times 2.0 \times 2.0$	3.37	1.21	–	2×18
Abdomen	T2w-TSE fatsat (respiration triggered)	Axial	$2.1 \times 1.5 \times 6.0$	242	4.13	–	57
	T1w-FLASH2D fatsat (multi breath-hold)	Axial	$1.6 \times 1.2 \times 6.0$	>3800	95	–	>106
Pelvis	T2w STIR-TSE	Axial	$1.5 \times 1.2 \times 4.0$	7100	70	150	271
After intravenous Gd-DTPA administration							
Brain	T1w-SE	Axial	$1.8 \times 1.3 \times 5.0$	400	7.8	–	228
	T1w-SE	Coronal	$0.9 \times 0.9 \times 4.0$	599	7.8	–	254
Neck	T1w-FLASH2D fatsat	Axial	$1.1 \times 0.8 \times 5.0$	554	4.13	–	75
Thorax	T1w-VIBE 3D (breath-hold)	Axial	$2.0 \times 2.0 \times 2.0$	3.37	1.21	–	2×18
Abdomen	T1w-FLASH2D fatsat (multi breath-hold)	Axial	$2.1 \times 1.5 \times 6.0$	242	4.13	–	57
Pelvis	T1w-FLASH2D fatsat	Axial	$2.1 \times 1.5 \times 4.0$	242	4.13	–	57

T2w STIR-TSE, T2-weighted short tau inversion recovery turbo spin echo; T1w-SE, T1-weighted spin echo; FLAIR, fluid attenuated inversion recovery; T1w-VIBE 3D breath-hold, T1-weighted volumetric interpolated, three-dimensional breath-hold; T2w-TSE, T2-weighted turbo-spin echo; T1w-FLASH, T1-weighted fast low angle shot; Gd-DTPA, Gadolinium-diethyltriaminepentaacetic acid.

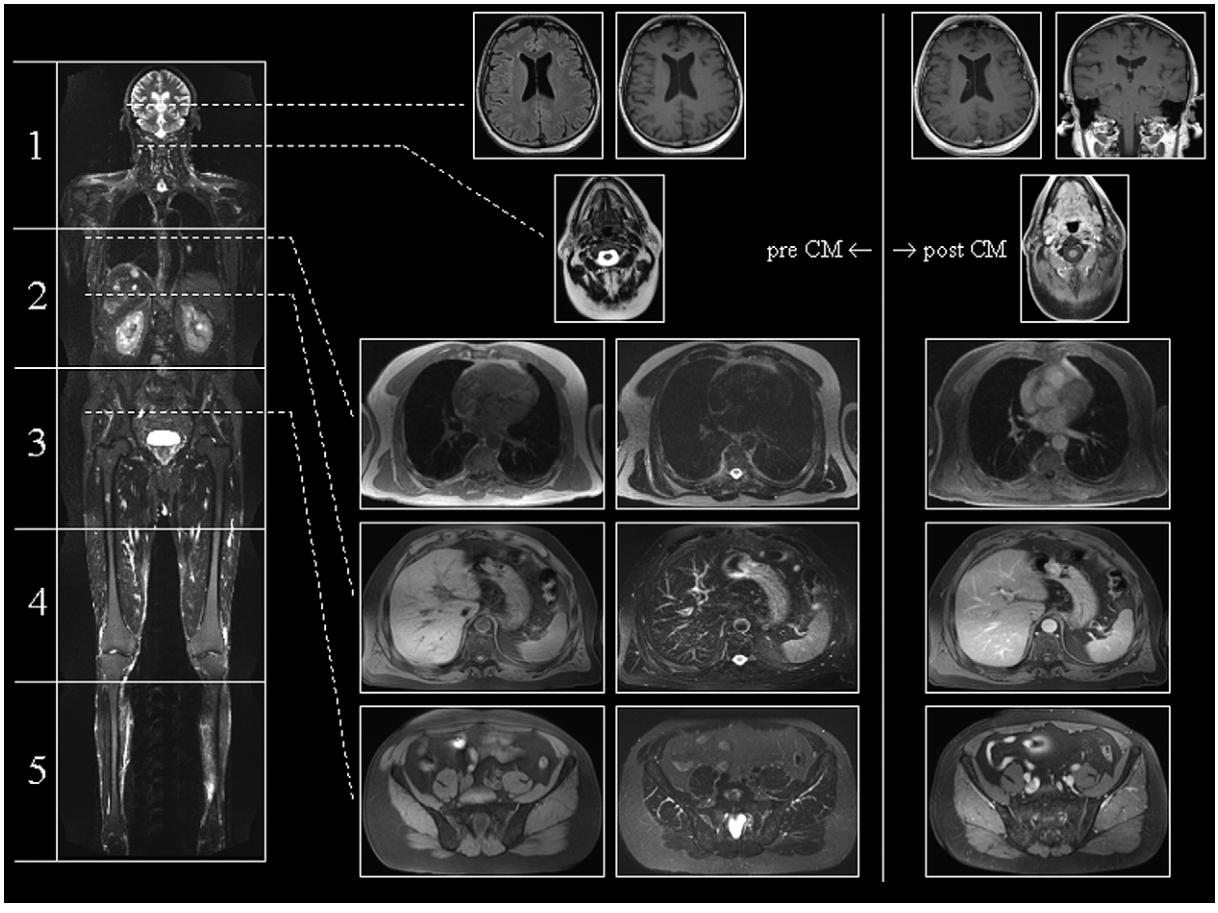

Fig. 1 – Example of a whole-body magnetic resonance imaging (wbMRI) examination (sequence parameters see Table 1).

2.4. Evaluation

Two experienced radiologists (11 years and 25 years of professional experience, respectively) interpreted the wbMRI and whole-body CT (wbCT) images independently without knowledge of respective findings. In case of differences in the reports of the two investigators, the images were reviewed again by both and a consensus on the interpretation of the images was obtained.

By using a two-point scale (metastasis/no metastasis), tumour suspicious lesions were documented in the following locations (lung, liver, spleen, kidneys, adrenal glands, subcutaneous fat, muscle, bone marrow and brain). CT and MR images were interpreted according to general radiological criteria. Metastases were characterised by areas with tumour suspicious shape, abnormal attenuation or signal and/or pathological enhancement after intravenous (i.v.) contrast medium. Similarly suspicious lymph nodes were documented in different draining regions (cervical/nuchal, axillar, mediastinal, hilar, mesenterial, retroperitoneal, pelvic/iliacal and inguinal). Most lymph nodes without metastatic involvement have an oval shape, whereas enlarged nodes appear round. A lymph node was rated as suspicious if its diameter was greater than 10 mm and its appearance was round. In case of malignant melanoma, malignant lymph nodes often have increased signal intensity on native T1-weighted images because melanin-containing cells decrease the T1-relaxation time. Consequently, MR also detected lymph nodes smaller than 10 mm, but with increased signal intensity on T1-weighted images these were rated as suspicious and the size was included in the evaluation. In this case, the size of the corresponding lymph node on CT images was also included in the evaluation. The largest diameter of each lesion displayed on CT and MRI was recorded and compared. If a lesion was detected only by CT (MRI) or MRI (CT), the diameter was noted as zero on MRI or CT, respectively.

The diameters of the lesions were registered in Sigma Plot® 2000 (SPSS Inc., Illinois, USA) in mm and then box plots from each organ were created. The median, 10th, 25th, 75th and 90th percentiles were plotted as vertical boxes with error bars. Additionally, all outliers above the 90th percentile or under the 10th percentile were plotted as crosshairs. In case the numbers of lesions were less than 6, only crosshairs of each lesion was plotted.

As each organ box plot was created separately from the lesions that were found with wbMRI as well as with wbCT (labelled 'MRI' and 'CT', respectively), from lesions that were only found with wbMRI (labelled 'MRI only') and from lesions that were only found with wbCT (labelled 'CT only'). In addition, the number of lesions is displayed above each box plot.

The number of patients with lesions in lung, liver, spleen, kidneys, adrenal glands, subcutaneous fat, muscle, bone marrow, and brain are illustrated in circle diagrams as percentages of the number of patients with lesions detected in wbMRI and wbCT (labelled 'MRI = CT'), more lesions with wbCT than wbMRI (labelled 'CT > MRI'), more lesions with wbMRI than in wbCT (labelled 'MRI > CT') and with lesions only detected by wbCT or wbMRI (labelled 'CT only' and 'MRI only').

Additionally, circle diagrams show the percentage of the number of the overall lesions from each organ over all patients, detected by wbCT as well as by wbMRI (labelled 'MRI = CT'), only detected by wbCT (labelled 'CT only') and only detected by wbMRI (labelled 'MRI only'). The mean diameter with standard deviation of the lesions is also depicted.

3. Results

Between February 2004 and October 2004, wbMRI and wbCT were performed successfully in 41/43 patients. Two patients refused the MRI examination due to claustrophobia. Thirty-seven of these 41 patients had cutaneous malignant melanoma and four patients had choroid malignant melanoma. A total of 775 metastases were identified by both methods in 41 patients. Whole-body CT was able to detect 522 metastases, whereas wbMRI found 730 metastases. Four patients were examined after excision of suspicious lymph nodes. No further tumour spread was found in these four patients using both CT and MRI. A complete overview of patients' characteristics is shown in Table 2 and the number of metastases according to different organ systems detected by wbCT and wbMRI scans is shown in Table 3.

3.1. Lung

Whole-body CT detected more lung metastases than wbMRI (Table 2). In 2/20 patients (10%) lung metastases were depicted by CT with a mean diameter of 5 ± 1 mm. All lung nodules larger than 5 mm were correctly identified using MRI. Whole-body CT detected more lung metastases than MRI in 6/20 patients (30%), but this had no impact on further therapy.

Table 2 – Patients' characteristics (n = 41)

Characteristics	Patients *n* (%)
Sex	
Male	24 (59)
Female	17 (41)
Age (years)	
0–40	5 (12.2)
41–50	7 (17.1)
51–60	10 (24.4)
>60	19 (46.3)
Clinical stage	
III	9 (22)
IV M1a	4 (9.7)
IV M1b	7 (17.1)
IV M1c	17 (41.5)
Not assessed	4 (9.7)
Organs involved	
Lung	20 (48.8)
Liver	19 (46.3)
Spleen	9 (22)
Kidneys	3 (7.3)
Adrenal glands	7 (17.1)
Subcutaneous tissue	12 (29.3)
Muscle	8 (19.5)
Bone marrow	13 (31.7)
Brain	9 (22)
Lymph nodes	27 (65.9)

Table 3 – Number of metastases according to different organ systems detected by whole-body computed tomography (wbCT) and whole-body magnetic resonance imaging (wbMRI) scans

Organ involvement	CT				MRI			
	Patients (*n*)	Metastases (*n*)	Size of metastases (mean ± SD) (mm)	Minimum/ maximum sizes (mm)	Patients (*n*)	Metastases (*n*)	Size of metastases (mean ± SD) (mm)	Minimum/ maximum sizes (mm)
Lung	20	188	9 ± 6	2/40	18	143	7 ± 7	3/40
Liver	16	122	12 ± 12	5/62	19	199	16 ± 11	3/65
Spleen	8	26	16 ± 11	5/61	9	54	8 ± 10	3/55
Kidneys	3	4	17 ± 8	10/30	3	4	16 ± 7	9/30
Adrenal glands	7	7	30 ± 8	20/41	7	7	30 ± 8	20/43
Subcutaneous tissue	10	39	12 ± 10	5/60	12	61	11 ± 9	3/64
Muscle	3	4	17 ± 23	38/60	8	11	33 ± 17	10/67
Bone marrow	5	23	3 ± 7	5/39	13	132	16 ± 12	5/105
Brain	7	15	8 ± 9	6/30	9	25	9 ± 7	2/28
Lymph nodes	26	94	19 ± 14	10/100	27	94	20 ± 19	10/100
Total number of metastases		522				730		

Except for the lung, MRI detected more or at least the same number of metastases in all examined regions than did CT. In total, 775 metastases were detected, which corresponds to 730 metastases detected by MRI plus 45 lung metastases detected only by CT.

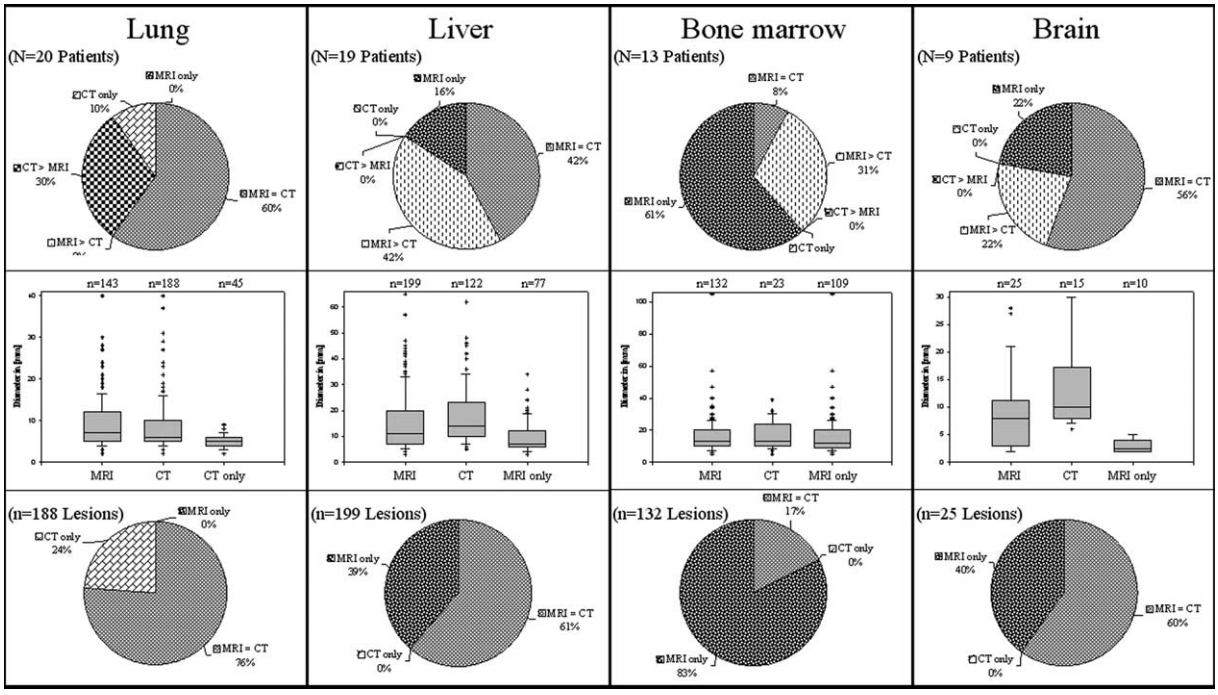

Fig. 2 – Upper row: Circle diagrams showing the percentage of the number of patients with detected lesions by magnetic resonance imaging (MRI) and computed tomography (CT), respectively. Middle row: Box plots showing lesion diameter. Horizontal bars indicate median, 10th, 25th, 75th and 90th percentiles of the lesions, outliers are plotted as crosshairs. Lower row: Circle diagrams showing the percentage of the number of all lesions detected by MRI and CT, respectively.

3.2. *Liver*

MRI was superior to CT in the detection of small liver metastases and was able to detect more lesions than CT in 8/19 patients (42%) (Figs. 2 and 3). In 3/19 patients (16%) the diagnosis of liver metastases was established only by MRI. The smallest lesion detected by MRI (CT) had a diameter of 3 (5) mm. MRI was particularly superior for the detection of small liver lesions with a mean diameter of 9 ± 5 mm.

3.3. *Spleen*

CT was able to detect 26/54 lesions (48%) in 6/9 patients (67%). In 2/9 patients (22%) MRI detected more lesions than CT and in 1/9 patients (11%) lesions were detected only by MRI.

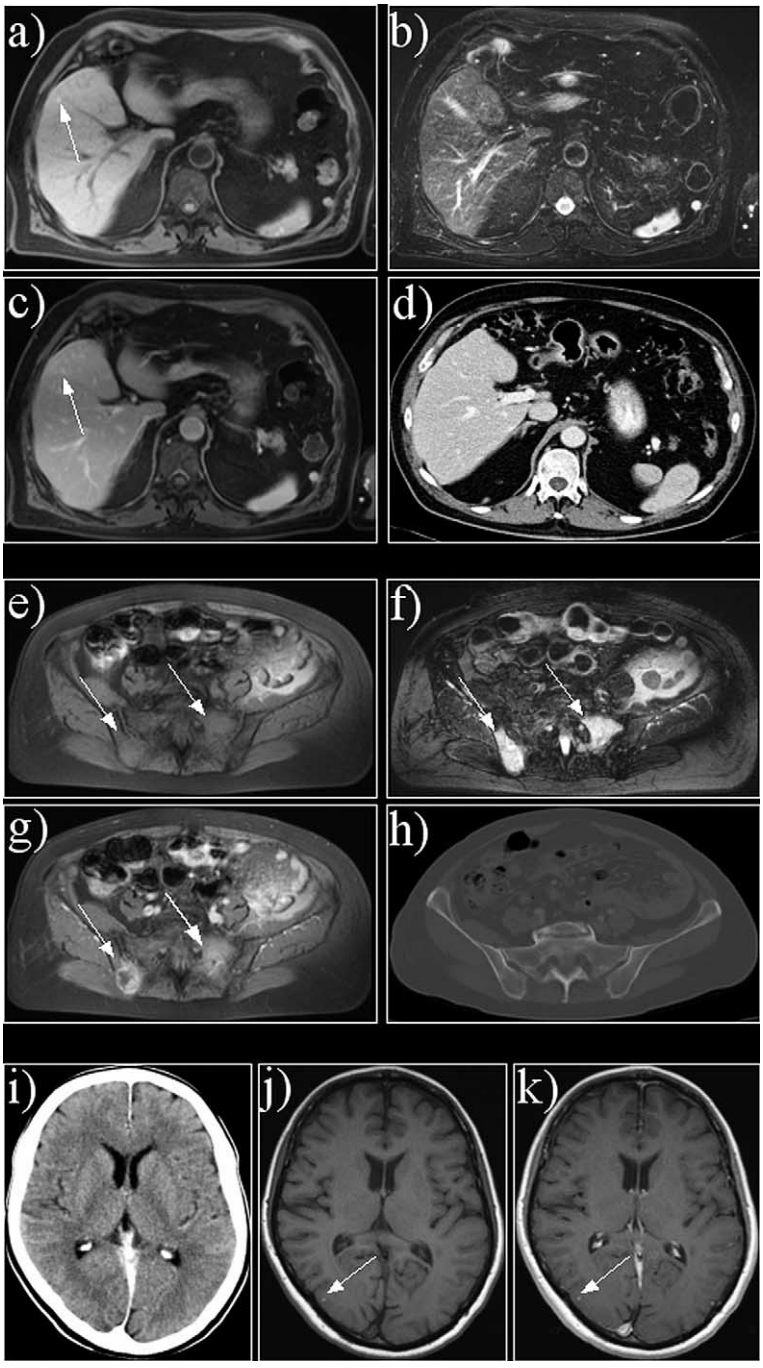

Fig. 3 – (a, e, j) T1-weighted magnetic resonance imaging (MRI), (b, f) T2-weighted MRI, (c, g, k) contrast-enhanced T1-weighted MRI and (d, h, i) contrast-enhanced computed tomography (CT) of three patients with liver metastases, with bone marrow involvement and with brain metastases. (a–d) In the first patient, only MRI shows a small (3 mm) liver metastasis not seen in the T2-weighted sequence and on CT. (e–h) In the second patient, only MRI shows a diffuse bone marrow infiltration of the pelvis. (i–k) In the third patient, only MRI shows a very small brain metastasis (3 mm).

3.4. *Kidneys and adrenal glands*

In kidneys and adrenal glands, MRI and CT were able to detect the same number of lesions in 3/41 and 7/41 patients, respectively.

3.5. *Subcutaneous metastases*

Sixty-one subcutaneous metastases in 12/41 patients were found by MRI. CT detected 39/61 (64%) in 4/12 patients (33%). In 6/12 patients (50%) MRI was able to detect more

lesions than CT and in 2/12 patients (17%) lesions were only detected by MRI.

3.6. Muscle

Eleven muscle metastases were detected by MRI in 8/41 patients. CT detected only 4/11 metastases (36%) in 2/8 patients (25%). In 1/8 patients (13%) MRI detected more lesions than CT and in 5/8 patients (62%) only MRI detected 7/11 metastases (64%).

3.7. Bone marrow

In bone marrow, 132 lesions in 13/41 patients were detected by MRI. CT detected 23/132 lesions (17%) in 5/13 patients (38%). In 4/13 patients (31%) MRI was able to detect more lesions than CT and in 8/13 (61%) only MRI detected 109/132 lesions (83%). Additionally, in 1/41 patients a diffuse infiltration of the pelvic bone marrow was only detected by MRI (Figs. 2 and 3).

3.8. Brain

In brain, MRI was able to detect 25 metastases in 9/41 patients. CT detected 15/25 metastases (60%) in 5/9 patients (56%). In 2/9 patients (22%) MRI was able to detect more metastases than CT and in 2/9 patients (22%) only MRI detected 10/25 metastases (40%) (Figs. 2 and 3).

3.9. Lymph nodes

A total of 97 suspicious lymph nodes were detected. In cervical/nuchal, axillar, inguinal, mesenterial and pelvic/iliacal region MRI and CT both detected the same number of metastatic lymph nodes. In mediastinal region MRI was able to detect six suspicious lymph nodes, whereas CT was only able to detect three of them. In the hilar region CT found 11 suspicious lymph nodes with a mean diameter of 22 ± 10 mm, whereas MRI was able to detect 8/11 only.

3.10. Modifications of treatment strategy due to wbMRI findings

The treatment plans were initially based on findings of conventional CT, which is usually performed for staging. The panel was allowed to change the treatment plan after disclosure of MRI results in an interdisciplinary conference consisting of dermatologists, surgeons, oncologists, radio oncologists and radiologists. So treatment modalities were modified as a consequence of wbMRI findings in 10/41 patients (24%). Three of them received bisphosphonates and one a palliative irradiation of the pelvis and the lumbar spine due to bone marrow metastases only detected by MRI. A chemotherapy schedule was applied to one patient prior to the wbMRI examination where a diffuse bone marrow infiltration of the pelvis was diagnosed. After the examination chemotherapy was discontinued and bisphosphonates were applied. In one patient suspicious lesions in liver were detected by wbCT and were classified as cysts and haemangiomas on wbMRI. Hence, no chemotherapy was applied. In another patient wbCT detected 1 liver lesion but wbMRI detected 5. In this case, a polychemotherapy instead of surgery was chosen as treatment. In the 8th patient wbMRI detected bone metastases in the spine and an emergency irradiation was performed because of imminent danger of paraplegia (Fig. 4). The 9th and 10th patients suffered from cerebral metastases, which were only detected by MRI. One of these patients had

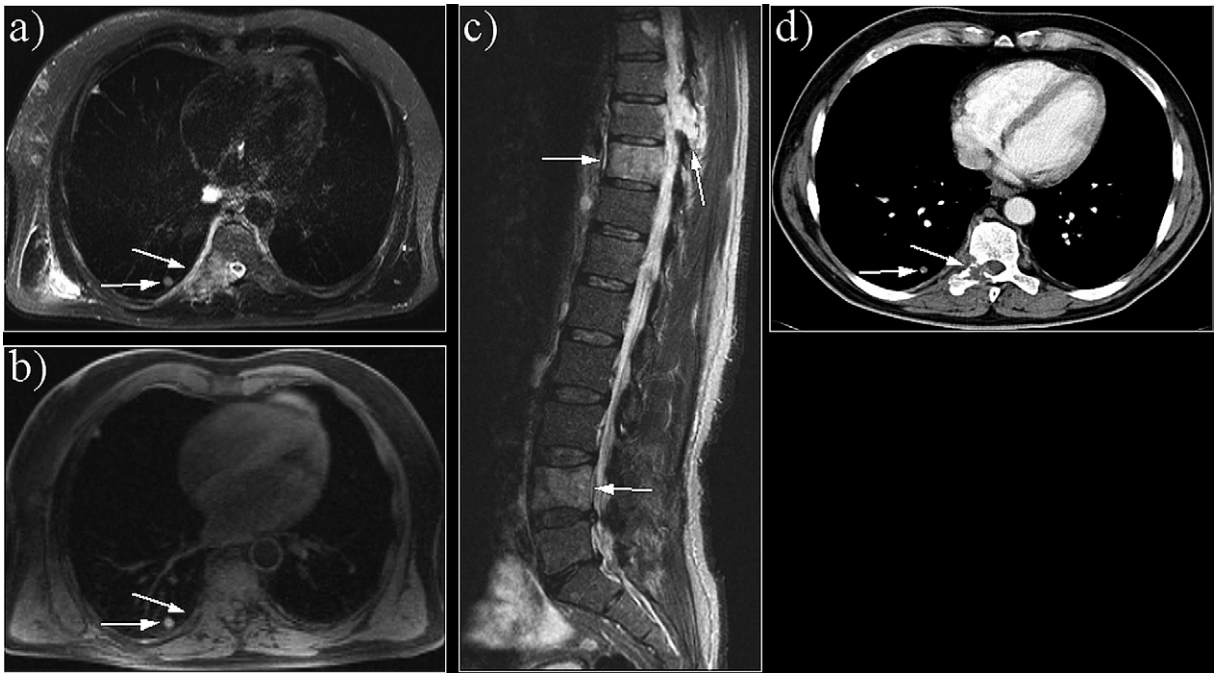

Fig. 4 – (b) T1-weighted magnetic resonance imaging (MRI), (a, c) T2-weighted MRI, (d) contrast-enhanced CT. A large metastasis of the vertebra body with infiltration of the surrounding soft tissue with a compress of the myelin is clearly depicted by MRI. A lung metastasis is shown by both methods.

only one metastasis measuring 5 mm, which was resected by surgery. The other patient had seven metastases, all <4 mm and irradiation of the whole brain was carried out.

4. Discussion

The primary objective of this study was to evaluate possible advantages of a wbMRI examination in comparison with a wbCT examination as a staging procedure for patients with advanced melanoma. The study proved that wbMRI is more sensitive in detection of metastases in parenchymal organs, particularly liver and brain as well as bone marrow involvement. Whole-body MRI is confirmed as an improvement in the diagnostic armamentarium.

The brain is rarely the initial site where solitary melanoma metastasis is identified [9]. Usually, CT scans and MRI of the brain do not show occult metastases in asymptomatic AJCC stage I, II and III patients [10]. However, Reider-Growasser and colleagues [11] have reported by means of CT scans AJCC stage IV in 2/28 patients with asymptomatic cerebral metastases. When brain metastases are suspected, MRI scan with gadolinium contrast is reported to be superior to the CT scan with contrast enhancement in detecting cerebral metastases and is clearly superior for metastases to the meninges and spinal cord. Median survival after complete surgical resection of brain metastases has been reported to be 5–15 months [12]. Commonly, brain metastases that could not be surgically resected are treated with whole-brain irradiation and/or gamma knife [13].

In liver very small metastases with diameters of 2 or 3 mm were only visible in the wbMRI because of their higher signal in the native T1-weighted (T1w) sequence due to melanin containing cells. Melanin-containing melanomas are displayed by high signal on T1w MRI. But small liver metastases from non-melanin-containing melanoma with 2–3 mm size can also be detected with wbMRI. Studies comparing wbMRI using the novel MRI system and wbPET-CT were currently performed and the results will be reported of the following studies.

Generally, bone marrow metastases occur in 11–17% of melanoma patients with widespread metastatic disease. In the present study we were able to confirm the superiority of wbMRI compared with wbCT in detecting bone marrow infiltration.

As in liver, wbMRI detected more metastases in spleen than wbCT because of the higher soft tissue contrast of wbMRI compared with CT. However, these findings did not affect treatment decisions.

Regarding metastases in kidneys and adrenal glands this study revealed no benefit of wbMRI in comparison with conventional CT.

In case of subcutaneous metastases, due to the lower soft tissue contrast of CT compared with MRI the lesions can easily be overlooked in the CT examination. However, those patients also suffered from lung and bone marrow metastases, the detection of additional subcutaneous metastases had no impact on the current treatment.

In muscle, MRI showed its superior soft tissue contrast compared with CT, but in all cases liver lesions or lung nodules were simultaneously found by CT and MRI. Therefore, we conclude that the higher sensitivity for the detection of muscle metastases by MRI was not associated with a clear advantage for the patients.

Lung metastases early in their development are frequently asymptomatic. The median survival time with pulmonary melanoma metastases is 8.3 months and the estimated 5-year survival rate is 3–4% [14]. Resection of solitary pulmonary metastases was reported to increase the median survival from 8–11 months to 17–31 months [12]. In several cases nodules of only 3 mm were also seen in wbMRI examination. However, 24% of the 199 nodules detected by CT were not visible on MRI. At present CT should still be the gold standard in detecting lung nodules. The clinical value of MRI for detecting pulmonary nodules is still under investigation [15].

The most common sites of malignant melanoma metastases in early metastases are near the site of the primary malignant melanoma in the skin, in the soft tissue, and in the regional lymph nodes. Their early detection may permit beneficial surgical therapy. Physical examination and ultrasound is best at detecting regional lymph node metastases [16]. However, metastases may be obscured by obesity, scarring or location in difficult-to-palpate anatomical sites. MRI is comparable to CT in identifying lymph nodes. Nevertheless, even quantitative assessment of signal intensity does not permit reliable follow-up of disease activity. In mediastinal region CT was able to detect only 50% of the suspicious lymph nodes. This may be due to the higher soft tissue contrast of MRI. On the other hand, in hilar region MRI gave a false negative in 3 of 11 nodes detected by CT. In this region pulsation artefacts often appear in MRI examination because of the vicinity of big vessels. Further studies should be carried out in order to examine whether wbMRI has advantages over PET-CT that can aid to determine the localisation of diseased lymph nodes and gives valuable information regarding the activity of residual tumour tissue.

Overall, this first prospective single-centre study clearly indicates the superiority of wbMRI over wbCT in detecting bone marrow involvement and small metastases in brain, liver and soft tissue. The technique was consequently well accepted by the referring physicians.

Follow-up examinations by wbMRI have the advantage, particularly in young patients, of avoiding high radiation doses (29% of the patients were 50 years old or younger). It is hoped that this novel method may additionally optimise the workflow in staging patients with solid tumours and reduce their hospitalisation time.

However, until now it is unclear whether wbMRI examinations will be cost effective, because the reimbursement for a wbMRI study is uncertain thus far and inconsistent for different institutions, and therefore can be only roughly estimated. Whole-body MRI costs about twice that of conventional wbCT and wbPET-CT about three times as much as normal wbCT.

Additionally, the availability of wbMRI scanners is presently much scarcer than CT scanners. The costs per examinations with CT are clearly lower than for MRI.

Another relatively new method in examining cancer patients is the PET-CT, which is, so far, the most expensive modality compared with CT and MRI. Prospective clinical studies have now to be planned in order to examine whether wbMRI examinations will have economic and medical benefits compared with CT and PET-CT.

It is of practical importance to define clearly the current role of wbMRI scanning in the staging and follow-up of melanoma and other solid tumours. It is probable that the method is too expensive to use in the primary staging or regular follow-up examinations of patients with low risk for recurrences. Hence, wbMRI examinations are particularly for patients with already known disseminated metastases, in whom the extent of metastasis and the kind of organ involvement influence the treatment strategy. Thus, the more accurate and complete staging information obtained by wbMRI is able to guide therapeutic decision-making.

In conclusion, wbMRI clearly proved to be more sensitive than wbCT for the detection of solid cancer metastasis; altogether, 41% more metastases were detected compared with the results of the wbCT technique. On the other hand, wbCT examination was more sensitive for the detection of lung metastases. The more accurate and complete staging by wbMRI had an impact on treatment strategy in about one-quarter of patients and influenced decisions on the indication for surgery, for radiation therapy, for chemotherapy and for administration of bisphosphonates. Therefore, patients may benefit from wbMRI examinations, allowing therapeutic decisions to be based on the most accurate staging information. To evaluate lung metastases, however, CT of the thorax should still additionally be performed.

REFERENCES

1. American Cancer Society. *Cancer facts & figures*. Atlanta: American Cancer Society; 2004. Available from: www.cancer.org/downloads/STT/CAFF_finalPWSecured.pdf.
2. Balch CM, Soong SJ, Gershenwald JE, et al. Prognostic factors analysis of 17,600 melanoma patients: validation of the American Joint Committee on Cancer melanoma staging system. *J Clin Oncol* 2001;**19**(16):3622–34.
3. Eigentler TK, Caroli UM, Radny P, et al. Palliative therapy of disseminated malignant melanoma: a systematic review of 41 randomised clinical trials. *Lancet Oncol* 2003;**4**(12):748–59.
4. Krown SE, Chapman PB. Defining adequate surgery for primary melanoma. *N Engl J Med* 2004;**350**(8):823–5.
5. Schlemmer HP, Schafer J, Pfannenberg C, et al. Fast whole-body assessment of metastatic disease using a novel magnetic resonance imaging system: initial experiences. *Invest Radiol* 2005;**40**(2):64–71.
6. Hargaden G, O'Connell M, Kavanagh E, et al. Current concepts in whole-body imaging using turbo short tau inversion recovery MR imaging. *Am J Roentgenol* 2003;**180**:247–52.
7. Antoch G, Vogt FM, Freudenberg LS, et al. Whole-body dual-modality PET/CT and whole-body MRI for tumor staging in oncology. *JAMA* 2003;**290**:3199–206.
8. Lauenstein TC, Goehde SC, Herborn CU, et al. Three-dimensional volumetric interpolated breath-hold MR imaging for whole-body tumor staging in less than 15 minutes: a feasibility study. *Am J Roentgenol* 2002;**179**(2):445–9.
9. Patel J, Didolkar M, Pickren J, et al. Metastatic pattern of malignant melanoma: a study of 216 autopsy cases. *Am J Surg* 1978;**135**:807–10.
10. Zartman GM, Thomas MR, Robinson WA. Metastatic disease in patients with newly diagnosed malignant melanoma. *J Surg Oncol* 1987;**35**:163–4.
11. Reider-Growasser I, Merimsky O, Karminsky N, et al. Computed tomography features of cerebral spread of malignant melanoma. *Am J Clin Oncol* 1996;**19**:49–53.
12. Houghton AN, Balch CM. Treatment for advanced melanoma. In: Balch CM, Houghton AN, Milton GW, Sober AJ, Soong S, editors. *Cutaneous melanoma*. 2nd ed. Philadelphia (PA): J.B. Lippincott; 1992. p. 468–97.
13. Radbill AE, Fiveash JF, Falkenberg ET, et al. Initial treatment of melanoma brain metastases using gamma knife radiosurgery: an evaluation of efficacy and toxicity. *Cancer* 2004;**101**(4):825–33.
14. Barth A, Wanek LA, Morton DL. Prognostic factors in 1521 melanoma patients with distant metastases. *J Am Coll Surg* 1995;**181**:193–201.
15. Biederer J, Both M, Graessner J, et al. Lung morphology: fast MR imaging assessment with a volumetric interpolated breath-hold technique: initial experience with patients. *Radiology* 2003;**226**(1):242–9.
16. Golder WA. Lymph node diagnosis in oncologic imaging: a dilemma still waiting to be solved. *Onkologie (Switzerland)* 2004;**27**(2):194–9.